

# Optical polarization observations in the Scorpius region: NGC 6124\*

M. Marcela Vergne,<sup>1,2,3</sup> Carlos Feinstein,<sup>1,2,3</sup> Ruben Martínez,<sup>1,3</sup>

Ana María Orsatti<sup>1,2,3</sup> and María Paula Alvarez<sup>1</sup>

<sup>1</sup>*Facultad de Ciencias Astronómicas y Geofísicas, Observatorio Astronómico, Paseo del Bosque, 1900 La Plata, Argentina*

<sup>2</sup>*Member of Carrera del Investigador Científico, CONICET, Argentina*

<sup>3</sup>*Instituto de Astrofísica de La Plata, CONICET*

10 November 2021

## ABSTRACT

We have obtained optical multicolour (UBVRI) linear polarimetric data for 46 of the brightest stars in the area of the open cluster NGC 6124 in order to investigate the properties of the interstellar medium (ISM) that lies along the line of sight toward the cluster. Our data yield a mean polarization efficiency of  $P_V/E_{B-V} = 3.1 \pm 0.62$ , i.e., a value lower than the polarization produced by the ISM with normal efficiency for an average colour excess of  $E_{B-V} = 0.80$  as that found for NGC 6124. Besides, the polarization shows an orientation of  $\theta \sim 8^\circ.1$  which is not parallel to the Galactic Disk, an effect that we think may be caused by the Lupus Cloud. Our analysis also indicates that the observed visual extinction in NGC 6124 is caused by the presence of three different absorption sheets located between the Sun and NGC 6124. The values of the internal dispersion of the polarization ( $\Delta P_V \sim 1.3\%$ ) and of the colour excess ( $\Delta E_{B-V} \sim 0.29$  mag) for the members of NGC 6124 seem to be compatible with the presence of an intra-cluster dust component. Only six stars exhibit some evidence of intrinsic polarization. Our work also shows that polarimetry provides an excellent tool to distinguish between member and non-member stars of a cluster.

**Key words:** ISM: dust, extinction,  
open clusters and associations: individual (NGC 6124)

## 1 INTRODUCTION

The open cluster NGC 6124 ( $l= 340.^{\circ}8$ ,  $b=+6.^{\circ}1$ ) is an intermediate-richness, detached cluster of slight concentration with stars in a wide range of brightness located in the Scorpius region. This cluster is seen as projected on the edge of a dust cloud which obscures some of its stars, on the north-western part of cluster area. NGC 6124 contains several red giant stars.

This cluster has been studied photoelectrically by Koelbloed (1959), but he only made rough estimates of the distance and of the age of the cluster. In order to get a more accurate determination of those parameters, the study of Koelbloed was extended photoelectrically and photographically to a fainter magnitude limit by Thé (1965). These initial studies of the cluster revealed important discrepancies between the values of the parameters that they obtained. Motivated by some evidence that this cluster is affected by differential reddening, Pedreros (1987) obtained a new set of UBV photoelectric observations for NGC 6124 and analyzed them using a reddening-line slope adequate for this region of the sky. The distance to NGC 6124 that he estimated using the less evolved stars is  $563 \pm 10$  pc. He also found an age of  $1.0 \times 10^8$  yr and a mean colour excess of  $E_{B-V} = 0.80 \pm 0.06$ .

A study of the interstellar polarization of NGC 6124 is warranted for three reasons: it provides information on the dust itself, it is a means to trace the galactic magnetic field and it is also useful to establish cluster membership. The comparison between the polarization and extinction values observed along the same line of sight provides tests for extinction models and grain alignment. The latter involves several processes acting simultaneously, but on different time-scales. The rotating dust grains get a substantial magnetic moment that allows them to precess rapidly about magnetic field lines and, as a result, the grains conserve their orientation relative to that of the magnetic field when the latter fluctuates, forcing the axes of the grains to be aligned with respect to the angular momentum of the grains (Lazarian and Cho 2005). Therefore, the observed polarization vectors map the projected direction of the magnetic field on the plane of the sky, and this allows the investigation of the structure of both the macroscopic field in our Galaxy (Mathewson and Ford 1970; Axon and Ellis 1976) and the local field associated with the individual clouds (Goodman et al. 1990).

Open Clusters are very good candidates for polarimetric observations, because many

\* Based on observations obtained at Complejo Astronómico El Leoncito (CASLEO), operated under agreement between the CONICET and the National Universities of La Plata, Córdoba, and San Juan, Argentina.

of them have been studied through photometric and spectroscopic techniques and detailed information on the colour, luminosity, spectral type, and other properties of their stars is readily available. Thus, the physical parameters of the cluster and its stars can be obtained, and adding polarimetric observations we can study the distribution, size and efficiency of the dust grains which polarize the starlight and the different directions of the galactic magnetic field along the line of sight to the cluster. As some of the open clusters spread over a significant area, it is possible to analyze the evolution of the physical parameters of the dust over the region. Besides, it is also possible to detect the presence (if any) of intra-cluster dust and, with additional observations of non-member stars in the same region, to investigate the interstellar dust distribution along the line of sight to the cluster. Finally, the polarimetric data can be used to detect the location of any energetic phenomenon that may have occurred in the history of a cluster (Feinstein et al. 2003), and very important by-products of these studies are the detection of stars displaying polarization of non-interstellar origin, such as stars with extended atmospheres (e.g., Be stars), and of dust associated to possible binary systems, or surrounding the stars (due to evolution or as a formation remnant).

Here we present multicolour (UBVRI) measurements of linear polarization vectors for stars observed in the direction to NGC 6124 and we use them to investigate the properties of the dust located along the line of sight to the cluster. In the following sections, we will discuss the observations, the data calibrations and the results obtained both for the individual stars and for the cluster as a whole.

## 2 OBSERVATIONS AND DATA REDUCTION

The linear optical polarimetry was obtained during several observing runs at the Complejo Astronómico El Leoncito (CASLEO) in San Juan, Argentina, during 2003-2007. The Torino five-channel photopolarimeter (Scaltritti et al. 1989, Scaltritti 1994) was used on the 2.15-m telescope. All observations were obtained simultaneously through the five Johnson-Cousins broad band UBVRI filters centered at  $\lambda_{Ueff} = 0.360 \mu m$ ,  $\lambda_{Beff} = 0.440 \mu m$ ,  $\lambda_{Veff} = 0.530 \mu m$ ,  $\lambda_{Reff} = 0.690 \mu m$  and  $\lambda_{Ieff} = 0.830 \mu m$ . Standard stars for null polarization and for the zero point of the polarization position angle were observed several times each night for calibration purposes. The instrumental polarization was obtained from the null polarization standards and subsequently used to correct the values derived for the program stars. Polarization standards were used to refer the observed polarization angles to

the equatorial system. Table 1 shows the average of the observations of the null polarization standards. Only in the last run a correction for instrumental polarization (hereafter: IP) on the U filter was needed. For the other filters the value of the IP was of the same order of magnitude of the observational errors which means that the IP is either negligible, or so low that it cannot be determined.

The polarimetric observations are listed in Table 2 which shows, in self explanatory format, the stellar identification as given by Koelbloed (1959), the polarization percentage ( $P_\lambda$ ) and the position angle of the electric vector ( $\theta_\lambda$ ) through each filter, as well as their respective mean errors computed considering the photon shot noise as the dominant source of errors (Maronna et al., 1992). Since the Torino photopolarimeter collects photons simultaneously in all the filters (UBVRI), the final data from each filter may be of different quality, especially those in the U band. Therefore, observations whose values were below the  $3\sigma$  level were ruled out and are not included in Table 2. Three stars (#6, 9, and 31) were not rejected, and are included in Table 2 although their measurements showed high errors, because they are evidently low polarization stars located near the Sun.

A total of 46 stars were polarimetrically observed in the area of NGC 6124. We have 21 stars in common with the photoelectric observations of Pedreros (1987) and other 6 stars that were quoted as red giants by Koelbloed (1959). The membership information for each star, indicated in the first column of Table 2, was obtained from Pedreros (1987), Thé (1965), Baumgard et al. (2000) and from the Webda (<http://www.univie.ac.at/webda/>). Note, however, that not all the stars observed for the present work have membership information.

### 3 RESULTS

The sky projection of the V-band polarization vectors for the observed stars in NGC 6124 are shown in Fig. 1. The dashed line superimposed to the figure is indicating the orientation of the projection of the Galactic Plane (GP), which has a P.A. of  $\theta_{GP} \sim 44^\circ$ . Most of the polarization vectors are not aligned with this direction. This is not the usual finding, because dust particles in most aged clusters are expected to have enough time to relax and polarize the light in the same orientation as the GP in the region (Axon et al., 1976). Normally this is a sign that a perturbation has happened to the dust (Ellis et al., 1978).

Fig. 2 shows the relation that exists between  $P_V$  and  $\theta_V$  for members (full points), red giants (starred symbols), non-members (open triangles) and stars without any membership

data (open circles). We can see a high scatter in angles, probably as a consequence of the presence of intra-cluster dust or a patchy structure of dust clouds on line of view to the cluster. Also, we observe a spread in polarization values of  $\Delta P_V = 1.3\%$  in the stars historically considered as members of the cluster (excluding stars 3 and 32 with low polarization values, whose memberships will be analyzed in the next sections).

Fig. 3 shows the polarization angle distribution. The majority of the stars have their angles in the range of  $-10^\circ < \theta_V < 20^\circ$  (grey bars) and the angle distribution of the polarization vectors of the members (dark bars) has a similar behaviour to that of the total sample, with a  $\Delta\theta_V > 20^\circ$  (with a  $FWHM \sim 8^\circ.5$ ). The mean orientation of the polarization vectors in the cluster is  $\bar{\theta}_V \sim 8^\circ.1$  (vertical dashed line) but the orientation of the GP in the region is  $\theta_{GP} \sim 44^\circ$  (vertical solid line). So both directions differ in  $\sim 36^\circ$  degrees. All the stars that have  $\theta_V > 25^\circ$  are already known non-members.

A group of 7 red giant stars (#1,14,29,33,35,36, and 41) is included in our sample, 6 of them photoelectrically observed by Koelbloed (1959). According to his data, they are K and M giants and members of the cluster. Pedreros (1987) adopted the photometric data from Koelbloed (1959) and their locations in his colour-colour diagram show that these stars would belong to the cluster. These evolved stars have extended atmospheres, therefore they are candidates to have a non-interstellar component in their polarizations. The polarization value, in the visualfilter, of each of the red giant stars is similar (see Table 2), excepting stars #1 and 41 that have extreme polarization values ( $P_V=3.75\%$  and  $P_V=1.58\%$ , respectively). The low polarization of the star #41 suggests that it could be depolarized due to the presence of an intrinsic component. The polarization angles of the giant stars are lower than  $10^\circ$ , with the exception of stars #33 and 36. The first one is classified as M0III in the literature, and according to Thé (1965) it can probably be a distant giant M star not belonging to the cluster. The second star (#36) has several spectral types in the literature (G2III, G8III, K2III), but according to the Washington Visual double catalog (Worley 1996), it has a companion with magnitude 14.20 mag. The binary nature of this star could explain the variation of the polarization angle with the wavelength.

## 4 ANALYSIS AND DISCUSSION

### 4.1 Serkowski’s Law

To analyze the data, the polarimetric observations in the five filters were fitted in each star of our sample using Serkowski’s law of interstellar polarization (Serkowski 1973). That is:

$$P_\lambda/P_{\lambda_{max}} = e^{-K\ln^2(\lambda_{max}/\lambda)} \quad [1]$$

We will assume that, if polarization is produced by aligned interstellar dust grains, the observed data (in terms of wavelength, UBVRI) will then follow [1] and each star will have a  $P_{\lambda_{max}}$  and  $\lambda_{max}$  values.

To perform the fitting we adopted  $K = 1.66\lambda_{max} + 0.01$  (Whittet et al. 1992). For all stars in the sample we computed the  $\sigma_1$  parameter (the unit weight error of the fit) in order to quantify the departure of our data from the “theoretical curve” of Serkowski’s law. In our scheme, when a star shows  $\sigma_1 > 1.5$ , it is indicating the presence of intrinsic stellar polarization. Also,  $\lambda_{max}$  values can be used to test the origin of the polarization: those stars which have  $\lambda_{max}$  much lower than the average value of the interstellar medium ( $0.545 \mu m$ , Serkowski, Mathewson and Ford 1975) are candidates to have an intrinsic component of polarization as well. Another criterion to detect intrinsic stellar polarization comes from computing the dispersion of the position angle for each star normalized by the average of the position angle errors ( $\bar{\epsilon}$ ). The values obtained for  $P_{\lambda_{max}}$ , the  $\sigma_1$  parameter,  $\lambda_{max}$ , and  $\bar{\epsilon}$  together with the identification of stars, are listed in Table 3. The expression used to calculate the  $\sigma_1$  parameter is also shown in the footnote. No star in Table 3 has its  $\lambda_{max}$  much lower than the average for the ISM.

Fig. 4 displays  $P_\lambda$  and  $\theta_\lambda$  plots for six stars (#13,26,27,36,42, and 46) with probable indications of intrinsic polarization. The presence of a non-interstellar component in the measured polarization of the light from a star causes a mismatch between observations and the Serkowski’s curve fit, and/or a rotation in the position angle of the polarization vector. This mismatch is clearly shown in the  $\sigma_1$  value for star #42 ( $\sigma_1 = 1.81$ ), and its variations in  $P_\lambda$  is a plane curve, indicating more than one component in polarization. In the other five stars, the presence of an intrinsic component of polarization is seen through the variation of  $\theta_\lambda$  ( $\bar{\epsilon}$  parameter). In particular, the  $P_U$  of star #36 is out of the Serkowski’s fit and, as it was mentioned before, it is a known binary system.

## 4.2 Stokes plane and memberships

To analyze the characteristics of the interstellar medium in the region of NGC 6124, we plot the normalized individual Stokes parameters in the visual filter of the polarization vector  $\vec{P}_V$ , given by  $Q_V = P_V \cos(2\theta_V)$  and  $U_V = P_V \sin(2\theta_V)$ , which represent the vector's equatorial components, for each of the observed stars. In this figure the stars are plotted according to the literature with their initial membership status. Filled circles are used for members, open triangles are used for non-members, starred symbols are used for red giant stars and open circles are used for those stars without membership information.

The polarimetric technique can help to solve membership problems. This type of plot ( $Q_V$  vs.  $U_V$ ) used in combination with photometric information is useful to separate between members and non-members.

In Fig. 5 the point of coordinates  $Q_V = 0$  and  $U_V = 0$  indicates the dustless solar neighborhood, and any other point represents the direction of the polarization vector with modulus  $P_V = \sqrt{Q_V^2 + U_V^2}$  as seen from the Sun. Again, this figure shows a high dispersion in angles.

### 4.2.1 Stars close to the Sun

On the left side of the diagram, near point (0,0), there is a group of three stars (#6,9,and 31) with very low polarization values (0.11%, 0.23% and 0.07%, respectively). Star 6 was observed by Pedreros (1987) and classified as a non-member of spectral type G5. Star 9, according to Thé (1965), may be a non-member variable star, and star 31 is of spectral type F8V (Houk et al. 1975). The low polarization of these stars is compatible with their small reddening. Therefore, they could be confirmed polarimetrically as non-member stars.

Stars #3 and 32 (originally considered as members) have their polarization values of 0.89 % and 1.02 %, respectively. From its photometric data, star 3 (of spectral type G2V) is located near the Sun ( $\sim 100$  pc), with an  $E_{B-V} = 0.08$  mag. compatible with its polarization. In Fig. 1 this star is projected on the north-west side of the sky, where a big dust cloud is observed, obscuring several members on this part of the cluster. Therefore, if it were a member, its light would be expected to be highly polarized, but it is not. For Star #32, according to its Q parameter (Schmidt-Kaler 1982), we obtain a F0-4V approximate spectral type and a distance of  $\sim 160$  pc. From these data, the polarization of the light of both stars

is likely caused in a dust cloud near the Sun, and for that we propose them as non-member stars.

#### 4.2.2 *Non-member stars*

In Fig. 5 there are two groups of non-member stars with different orientations of polarization vectors, but with similar values in polarization. There is a group made up of 4 non-member stars (#34,39,44 and 45) with mean values  $\bar{\theta}_V=17^\circ$  and  $\bar{P}_V=1.98\%$ . Koelbloed (1959) suggested that #44 and #45 were members of the cluster with a common spectral type AO, but their reddenings are smaller than those of other A type stars in the main sequence of the cluster; and besides, #44 is a B8II star according to Houk et al. (1975). Also, if we take into account that these four stars are very close in projection on the sky (on the west size, see Fig. 1) and in the  $Q_V-U_V$  plane, indicating similar polarimetric characteristics, probably they are polarized by the same dust cloud. From their photometric data, they are situated nearby the cluster ( $\sim 400$  pc from the Sun) and in front of it. Therefore, we may confirm them polarimetrically as foreground non-member stars. Also, stars #36 (red giant) and #42 (member) could form part of this group, but they show some evidence of a non-interstellar component.

Other two non-member stars, #20 and 28, have very different polarimetric orientations ( $2^\circ.7$  and  $0^\circ.8$ , respectively) in comparison to the preceding non-members. Both stars are projected on the central part of the cluster (Fig. 1), and to a mean distance of the Sun of approximately 200 pc (from their photometric data). The scatter between the two non-member groups in their position angles ( $\Delta\theta_V \sim 16^\circ$ ) may be showing that the light from these stars is polarized by several overlapped dust components along the line of sight to the cluster, with different orientations of the local magnetic fields.

#### 4.2.3 *Cluster stars*

Most stars in our sample have their  $Q_V$  values in the range (1.29, 2.6), with a high scatter in polarization angles. In this range we observe a group of stars showing some degree of concentration, considered most of them as members in the literature. To derive mean values, in angle and polarization for the cluster, we use seven member stars (#8,18,21,30,37,38, and 40), obtaining  $\bar{P}_V=2.11\%$  and  $\bar{\theta}_V=8^\circ.2$ . The wavelength of maximum polarization for the same group of stars amounts to  $\bar{\lambda}_{max} = 0.57 \pm 0.04 \mu\text{m}$ , a value very close to that of the ISM.

According to their locations on the  $Q_V-U_V$  plane stars #22 and 26 (originally non-members) may be polarimetrically considered now as members.

On the upper side of this group, we find three stars #5,33, and 43 with polarization values higher than the mean value for the cluster ( $P_V=2.77\%$ ,  $2.78\%$ , and  $2.7\%$ , respectively). Star #5, of spectral type B6II/III (Houk et al 1975), is considered as a member by Pedreros (1987), with a 60% of membership probability (Baumgardt et al. 2000). Polarimetrically, it shows characteristics in angle similar to the members of the cluster, in spite of its high polarization value. Its estimated distance, according to the spectral type, is approximately of 570 pc. As mentioned before, star #33 has a spectral type M0III and probably it is a distant giant not belonging to the cluster. Star #43 (spectral type B2III-IV) is considered a member with a membership probability of 77% (Baumgardt et al. 2000), but the orientation of the polarization vector ( $\theta_V=18^\circ.1$ ) is very different from the mean value of the cluster. As this star is an evolved object, an intrinsic polarization component may be expected, but our indicators do not show it. Therefore, these three stars may be possible non-members, due to their position in the  $Q_V-U_V$  plane.

Stars #11, 12, 13 and 16 are located on the lower side of the  $Q_V-U_V$  plane. Star #16 is considered as a member by Pedreros (1987), but its polarization value ( $1.63\%$ ) and orientation ( $\theta_V=176^\circ$ ) are both lower than the corresponding values of the rest of members. The estimated spectral type for this star, based on photometric data, gives A8V with a  $E_{B-V}=0.39$  mag. and a distance to the Sun smaller than that of the cluster. In Fig. 1, it lies near stars #20, and #28 on the central part of the cluster, and also in the  $Q_V-U_V$  plane, which indicates similar polarimetric characteristics in the dust causing the polarization. Polarimetrically, we conclude that star #16 may be a non-member in front of NGC 6124. Stars #11 and 12 have no membership information, and there is a lack of (U-B) values, therefore it cannot make any prediction about it. Polarimetrically, star #11 has a high polarization value to be considered a member, and the orientation of the polarization vector in the star #12 is very different from the  $\bar{\theta}_V$  for the cluster. Star #13 displays intrinsic polarization, and its location in the  $Q_V-U_V$  plane is clearly of a non-member.

#### 4.2.4 Background Stars

On the right side of the same figure, it can be seen three stars (#1,2 and 4) which are the most polarized in our sample with  $P_V = 3.36\%$ ,  $3.42\%$  and  $3.35\%$  respectively. On the

sky plane (Fig. 1), they are located on the west side of the cluster and to the south of a big dust cloud. Their polarization angles ( $\theta_V=6^\circ.4$ ,  $4^\circ.8$ , and  $8^\circ.7$ , respectively) are similar to the mean value of the cluster. Star 1 was classified as G8III; therefore, it should have  $E_{B-V} = 0.87$  mag. Originally, it was considered as a member by Pedreros(1987), but its membership probability is lower than 50% (Baumgardt et al. 2000). The other two stars have not membership information. The location of these three stars in the  $Q_V$  vs.  $U_V$  plot shows characteristics of background stars, their light being polarized for a dust component between them and the cluster.

### 4.3 Polarization efficiency and distribution of interstellar matter

The ratio  $P_V/E_{B-V}$  is known as the "polarization efficiency" of the interstellar medium and it depends mainly on the alignment efficiency, the magnetic field strength and the depolarization due to radiation traversing more than one dust cloud with different field directions.

Fig. 6 displays the relation ( $P_V$  vs.  $E_{B-V}$ ) that exists between the reddening and the polarization produced by the dust grains along the line of sight to NGC 6124. Assuming normal interstellar material characterized by  $R=3.2$ , the empirical upper limit relation for the polarization efficiency given by  $P_V = RA_V \sim 9E_{B-V}$  (Serkowski et al. 1975) is depicted by the solid line in this figure. Indeed, this line represents the maximum efficiency of the polarization produced by the interstellar dust. Likewise, the dotted line  $P_V = 3.5E_{B-V}^{0.8}$  represents the most recent estimate of the average efficiency made by Fosalba et al. (2002), valid for  $E_{B-V} < 1.0$  mag. The dashed line  $P_V = 5E_{B-V}$  was drawn as a reference and represents the observed normal efficiency of the polarizing properties of dust given by Serkowski et al. (1975). In this figure the stars are plotted with our polarimetric membership status.

Excesses  $E_{B-V}$  were obtained from the literature or from the relation between spectral type and colour index following Schmidt-Kaler (1982). In Fig. 6 the majority of stars lie on the right of the interstellar maximum efficiency line ( $P_V/E_{B-V} \sim 9$ , Serkowski et al., 1975), indicating that the observed polarization is mostly due to the ISM. Only two stars (#3,28) lie on the left of the line; this can be associated with errors in the estimate of their excesses.

To derive the mean polarimetric efficiency, we made use of the same 7 stars that we selected to calculate the mean polarization and angle of NGC 6124 (section 4.2), located around the cross symbol in Fig. 6. We obtained a mean efficiency  $P_V/E_{B-V}=3.1\pm 0.62$ ,

which is smaller than the value for the interstellar dust given by the Fosalba's estimate ( $P_V/E_{B-V} \sim 3.66$ ) and still much smaller than the value given by the Serkowski's estimate ( $P_V/E_{B-V} \sim 5$ .) for the average efficiency.. This depolarization in the cluster can be the result of the superposition of several dust clouds on the line of sight with different magnetic field directions, confirming the information given in section 4.1. Also, it shows scattering in colour excess (approximately  $0.60 < E_{B-V} < 0.89$ ) and in the polarization values ( $\Delta P_V \sim 1.3\%$ ) between members of the cluster. This may be a consequence of the presence of intra-cluster dust.

Star #32 on the lower side of the figure is probably a late-type star, whose excess may be overestimated. This star is marked in the plot using an arrow that points to smaller excesses. Stars #1 and #33 show low  $E_{B-V}$ s according to the polarization values. Polarimetrically, they are non-member stars with erroneous  $E_{B-V}$ s due to their bad photographic photometry. Again, as mentioned in the preceding section, star #22 shows polarimetric characteristics of a member of the cluster.

In all stars without membership data it was not possible to calculate their colour excesses. It is the situation for #2,7,10,11,12,17,23,24,25,27,31, and 46. In the case of stars #7, 12, and 24, they may be considered new probable members of NGC 6124, as their  $P_V$  values are similar to those associated with cluster stars. Also, they are located in the region of the  $Q_V$  vs.  $U_V$  plane where there is a number of members. The rest of stars may be probably in the background (like 2 and 11) or nearby non-members (between the Sun and the cluster) like #10,17,23,25,27,31, and 46.

#### 4.4 Dust clouds

Our data show that the orientation of the polarimetric vectors is not parallel to the Galactic Plane (Axon et al., 1976), and that there is a considerable degree of depolarization. These two properties can be explained by the composition of the individual effects of several clouds along the line of sight to the cluster, where at least one of these layers of dust polarizes the starlight in an orientation different than the rest, resulting in depolarization. That unusual component might have been recently perturbed so that their dust particles might have not had enough time to relax and to orient in the direction of the Galactic Plane. The most likely candidate to explain this polarimetric component (and its properties) is the Lupus cloud.

NGC 6124 lies behind the Lupus cloud which is a large structure composed of several sub-clouds showing different modes of star formation. Applying a maximum-likelihood technique to Hipparcus data, Lombardi et al. (2008) obtained a distance of  $d=155\pm 8$  pc, confirming the historical estimate of  $d\sim 150$  pc. The subcloud known as Lupus 6 is close to the direction of NGC 6124. The cluster is behind a long dark filament that crosses Lupus 6 and continues up to Lupus 4. Feinstein et al. (2003) have shown that, over the region of NGC 6231, the Lupus cloud does not polarize the light parallel to the Galactic Plane. The Lupus cloud also stands out as a strong and compact perturbation of the optical polarization of the Galaxy in Figs. 1b and 1c of Axon et al. (1976).

Three non-member stars in the region which seem to be polarized by the Lupus cloud, (#16, 20, and 28) give the mean values  $\bar{P}_V \sim 1.6\%$  and  $\bar{\theta}_V \sim 0^\circ$ . The combination of this orientation and that of the Galactic Plane ( $\theta_V \sim 44^\circ$ ), close to  $90^\circ$  in the  $Q_V - U_V$  plot, could explain the high depolarization of the data. Besides, it could explain the spread of the observations along the  $Q_V$  axis (where  $\theta_V \sim 0^\circ$ ), for all lowly polarized stars. As expected, the polarization caused by the Lupus cloud on NGC 6124 is not exactly the same as that for NGC 6231, because the cloud changes its optical properties between the two clusters. In the case of NGC 6231, the observed polarizations for stars #102 and 189 (suspected to be polarized by Lupus), are  $P_V=0.85\% \pm 0.10$ ,  $\theta_V=8^\circ.0 \pm 3.3$  and  $P_V=0.46\% \pm 0.11$ ,  $\theta_V=18^\circ.4 \pm 6.9$  respectively, i.e. somewhat similar in angle, but lower in polarization percentage, to the mean results for the three non-member stars in the NGC 6124 region.

Fig. 7 shows the trend of absorption ( $\bar{A}_V$ ) with increasing distance in the area of NGC 6124. Only stars whose distances were obtained by us are included, and the dot-dashed line accounts for the presence of three absorption sheets between the Sun and NGC 6124 ( $d\sim 560$  pc). The first dust component is located very near the Sun and affects stars #3 and #32, but does not produce much extinction ( $A_V=0.2$ ). Farther out, the absorption increases at about 160 pc (second absorption sheet) as it could be expected from the presence of the Lupus cloud where stars #20 and #28 are located ( $A_V \sim 0.5$  mag.). Between approximately 200 and 400 pc there are no stars with known distances, but from 400 pc up to the cluster location Fig. 7 shows that the extinction increases considerably, perhaps due to the presence of several dust clouds along the line of sight to the cluster, as mentioned in the preceding sections. A step in the absorption value within the cluster itself can be also noticed and it is probably caused by the presence of an intracluster dust component.

## 5 SUMMARY

We obtained the linear polarization of a sample of 46 stars in the region of the open cluster NGC 6124. Through the analysis of our polarimetric data, we have found evidence for at least three dust layers along the line of sight to the cluster.

The average polarization has an angle of  $\bar{\theta}_V=8^\circ.2$  which is not parallel to the Galactic Plane, and the mean polarization efficiency is  $P_V/E_{B-V}=3.1$ . This value is lower than the average polarization efficiency for the interstellar medium, which means that the cluster is highly depolarized. The scatter in polarization ( $\Delta P_V \sim 1.3\%$ ) and in extinction ( $\Delta E_{B-V} \sim 0.29$  mag.) for the members of the cluster are compatible with the presence of intra-cluster dust.

Our data show that one of these components is associated with the Lupus cloud, and that it polarized the light close to  $\theta_V=0^\circ$ . This orientation differs from the Galactic Plane projection in the region ( $\theta_{GP}=44^\circ$ ). We interpret that these two different directions of polarizations tend to depolarize the light from the cluster stars, because in the  $Q_V - U_V$  plane it is basically  $2\theta \sim 90^\circ$ .

We have shown that polarization measurements are useful to detect the non-member stars that contaminate the sample in the NGC 6124 region, and we have been able to detect a few stars with intrinsic polarization.

## ACKNOWLEDGMENTS

We wish to acknowledge the technical support at CASLEO during the observing runs. We also acknowledge the use of the Torino Photopolarimeter built at Osservatorio Astronomico di Torino (Italy) and operated under agreement between Complejo Astronómico El Leoncito and Osservatorio Astronomico di Torino. We thanks Dr. Juan Carlos Muzzio for reading of the manuscript and for his useful comments that helps to improve this paper. This research has made use of the WEBDA database, operated at the Institute for Astronomy of the University of Vienna.

## REFERENCES

- Axon, D.J., Ellis, R.S. 1976, MNRAS, 177,499  
 Baumgardt, H., Dettbam, C., Wielen, R. 2000, A&AS, 146, 251  
 Ellis, R.S., Axon, D.J. 1978, Astrophysics and Space Science, 54,425  
 Feinstein, C., Martínez, R., Vergne, M. M., Baume, G., Vázquez, R. 2003, ApJ, 598,349

- Fosalba, P., Lazarian, A., Prunet, A., Tauber, J. 2002, ApJ, 564,762
- Goodman, A. A., Bastien, P., Myers, P. C., Menard, F. 1990, ApJ, 359,363
- Houk N., Cowley A.P., Smith-Moore M. 1975, University of Michigan Catalogue of two-dimensional Spectral Types for the HD stars (Ann Arbor: Univ.of Michigan), Vol. 1
- Koelbloed, D. 1959, Bull. Astron. Inst. Netherlands, 14,265
- Lazarian, A., Cho, J. 2005, ASPC, 343,333
- Lombardi, M., Lada, C. J., Alves, J. 2008, A&A, 480, 785
- Maronna, R., Feinstein, C., Clocchiatti, A. 1992, A&A, 260,525
- Mathewson, D. S., Ford, V. L. 1970, MemRAS, 74,139
- Pedreras, M., 1987, AJ, 94,1237
- Scaltriti, F., Piirola, V., Cellino, A., Anderlucci, E., Corcione, L., Massone, G., Racciopi, F., & Porcu, F. 1989, Mem.S.A.It 60, 1-2
- Scaltriti, F. 1994, Technical Publication N° TP-001, Osservatorio Astronomica di Torino
- Schmidt-Kaler, Th. 1982, Landolt-Borstein, Numerical Data and Functional Relationships in Science and Technology New Series, Group VI, Vol. 2, eds. K. Schaifers and H. H. Voigt (Berlin, Springer-Verlag)
- Serkowski, K. 1973, in IAU Symp. 52, Interstellar Dust and Related Topics, ed. J. M. Greenberg H. C. van de Hults (Dordrecht:Reidel), p. 145
- Serkowski, K., Mathewson, D. L., Ford, V. L. 1975, ApJ, 196,261
- Thé, P. S. 1965, Contr. Bosscha Obs. Nr. 33
- Whittet, D. C. B., Martin, P. G., Hough, J. H., Rouse, M. F., Nailey, J. A., Axon, D. J. 1992, ApJ, 386,562
- Worley, C. E., Douglass, G. G. 1996, A&AS, 125, 523

**Table 1.** Results for zero polarizations standards

Date Number of observations	U	B	V	R	I
	$Q_U(\%) \pm \epsilon_{Q_U}$ $U_U(\%) \pm \epsilon_{U_U}$	$Q_B(\%) \pm \epsilon_{Q_B}$ $U_B(\%) \pm \epsilon_{U_B}$	$Q_V(\%) \pm \epsilon_{Q_V}$ $U_V(\%) \pm \epsilon_{U_V}$	$Q_R(\%) \pm \epsilon_{Q_R}$ $U_R(\%) \pm \epsilon_{U_R}$	$Q_I(\%) \pm \epsilon_{Q_I}$ $U_I(\%) \pm \epsilon_{U_I}$
29 April-2 May 2003	$0.08 \pm 0.13$	$0.10 \pm 0.12$	$0.02 \pm 0.06$	$0.02 \pm 0.08$	$0.03 \pm 0.07$
12	$-0.08 \pm 0.2$	$-0.06 \pm 0.13$	$-0.06 \pm 0.131$	$0.01 \pm 0.16$	$-0.07 \pm 0.15$
18-20 April 2004	$-0.12 \pm 0.09$	$0.06 \pm 0.04$	$-0.02 \pm 0.02$	$-0.001 \pm 0.02$	$-0.011 \pm 0.05$
5	$0.02 \pm 0.15$	$0.03 \pm 0.05$	$0.05 \pm 0.07$	$0.002 \pm 0.03$	$0.006 \pm 0.05$
21-24 May 2007	$-0.24 \pm 0.01$	$-0.01 \pm 0.01$	$-0.09 \pm 0.07$	$-0.03 \pm 0.05$	$-0.04 \pm 0.05$
6	$-0.190 \pm 0.03$	$-0.08 \pm 0.02$	$0.03 \pm 0.06$	$0.006 \pm 0.07$	$0.012 \pm 0.14$

**Table 2.** Polarimetric Observations of stars in NGC 6124

Star Id. Filter	$P_\lambda \pm \epsilon_P$ %	$\theta_\lambda \pm \epsilon_\theta$ °
Star 1 (rg)		
U	$2.91 \pm 0.69$	$2.4 \pm 6.7$
B	$4.05 \pm 0.31$	$8.4 \pm 2.2$
V	$3.36 \pm 0.23$	$6.4 \pm 2.0$
R	$3.74 \pm 0.21$	$4.9 \pm 1.6$
I	$3.30 \pm 0.28$	$4.0 \pm 2.4$
Star 2		
U	$2.95 \pm 0.15$	$3.3 \pm 1.4$
B	$3.67 \pm 0.14$	$3.9 \pm 1.1$
V	$3.42 \pm 0.26$	$4.8 \pm 2.2$
R	$3.44 \pm 0.17$	$4.5 \pm 1.4$
I	$3.18 \pm 0.20$	$5.8 \pm 1.8$
Star 3 (m)		
U	$0.77 \pm 0.17$	$13.7 \pm 6.2$
B	$0.92 \pm 0.09$	$15.0 \pm 2.7$
V	$0.89 \pm 0.08$	$15.1 \pm 2.5$
R	$0.98 \pm 0.08$	$13.1 \pm 2.2$
I	$0.90 \pm 0.10$	$13.9 \pm 3.1$
Star 4		
U	$2.54 \pm 0.30$	$15.2 \pm 3.4$
B	$3.46 \pm 0.16$	$11.2 \pm 1.3$
V	$3.35 \pm 0.14$	$8.7 \pm 1.2$
R	$3.56 \pm 0.10$	$9.4 \pm 0.8$
I	$3.13 \pm 0.12$	$8.8 \pm 1.1$
Star 5 (mP)		
U	$2.25 \pm 0.22$	$13.3 \pm 2.8$
B	$2.68 \pm 0.17$	$11.2 \pm 1.8$
V	$2.77 \pm 0.15$	$12.2 \pm 1.5$
R	$2.70 \pm 0.12$	$11.4 \pm 1.3$
I	$2.62 \pm 0.15$	$10.4 \pm 1.6$
Star 6 (nP)		
U	$0.46 \pm 0.33$	$56.6 \pm 17.7$
B	$0.23 \pm 0.27$	$83.4 \pm 24.7$
V	$0.11 \pm 0.34$	$82.6 \pm 36.0$
R	$0.08 \pm 0.17$	$92.1 \pm 32.0$
I	$0.14 \pm 0.20$	$66.2 \pm 27.7$
Star 7		
U	$2.05 \pm 0.28$	$8.5 \pm 3.8$
B	$2.33 \pm 0.25$	$10.4 \pm 3.0$
V	$2.09 \pm 0.32$	$13.0 \pm 4.3$
R	$2.03 \pm 0.22$	$12.7 \pm 3.0$
I	$1.73 \pm 0.25$	$7.8 \pm 4.1$
Star 8 (mP)		
U	$1.67 \pm 0.19$	$13.0 \pm 3.3$
B	$2.09 \pm 0.13$	$8.6 \pm 1.7$
V	$1.95 \pm 0.12$	$9.6 \pm 1.7$
R	$2.02 \pm 0.10$	$9.4 \pm 1.5$
I	$1.75 \pm 0.14$	$8.3 \pm 2.3$
Star 9 (n)		
U	$0.65 \pm 0.34$	$57.9 \pm 13.8$
B	$0.19 \pm 0.18$	$42.5 \pm 22.4$
V	$0.23 \pm 0.13$	$99.6 \pm 14.5$
R	$0.05 \pm 0.12$	$130.4 \pm 33.0$
I	$0.09 \pm 0.17$	$160.1 \pm 31.4$

Table 2. continued

Star Id. Filter	$P_\lambda \pm \epsilon_P$ %	$\theta_\lambda \pm \epsilon_\theta$ °
Star 10		
U	$1.67 \pm 0.36$	$0.1 \pm 6.1$
B	$1.87 \pm 0.32$	$5.3 \pm 4.8$
V	$1.76 \pm 0.34$	$8.2 \pm 5.5$
R	$1.71 \pm 0.21$	$11.3 \pm 3.5$
I	$1.62 \pm 0.29$	$13.5 \pm 5.1$
Star 11		
U	$2.60 \pm 0.22$	$179.6 \pm 2.4$
B	$2.88 \pm 0.10$	$0.6 \pm 1.0$
V	$3.03 \pm 0.15$	$178.9 \pm 1.4$
R	$3.04 \pm 0.11$	$178.8 \pm 1.0$
I	$2.72 \pm 0.17$	$177.9 \pm 1.8$
Star 12		
U	$2.06 \pm 0.56$	$5.9 \pm 7.6$
B	$2.06 \pm 0.17$	$177.3 \pm 2.3$
V	$2.44 \pm 0.27$	$173.6 \pm 3.2$
R	$2.48 \pm 0.23$	$174.6 \pm 2.7$
I	$2.05 \pm 0.27$	$174.6 \pm 3.8$
Star 13 (nP)		
U	$1.53 \pm 0.25$	$4.1 \pm 4.6$
B	$1.84 \pm 0.19$	$1.4 \pm 3.0$
V	$1.76 \pm 0.22$	$170.5 \pm 3.6$
R	$1.90 \pm 0.19$	$172.3 \pm 2.9$
I	$1.65 \pm 0.22$	$168.7 \pm 3.7$
Star 14 (rg)		
U	$3.41 \pm 0.87$	$12.0 \pm 7.1$
B	$2.44 \pm 0.29$	$7.6 \pm 3.4$
V	$2.52 \pm 0.26$	$5.8 \pm 3.0$
R	$2.64 \pm 0.22$	$7.4 \pm 2.4$
I	$2.18 \pm 0.28$	$6.5 \pm 3.6$
Star 15 (mP)		
U	$2.29 \pm 0.28$	$178.6 \pm 3.5$
B	$2.44 \pm 0.16$	$3.0 \pm 1.8$
V	$2.53 \pm 0.18$	$1.6 \pm 2.0$
R	$2.68 \pm 0.13$	$2.2 \pm 1.4$
I	$2.25 \pm 0.16$	$0.3 \pm 2.1$
Star 16 (mP)		
U	$1.31 \pm 0.30$	$176.6 \pm 6.5$
B	$1.58 \pm 0.09$	$177.6 \pm 1.6$
V	$1.54 \pm 0.11$	$176.0 \pm 2.1$
R	$1.60 \pm 0.09$	$175.1 \pm 1.6$
I	$1.41 \pm 0.13$	$173.9 \pm 2.6$
Star 17		
U	$1.94 \pm 0.51$	$6.6 \pm 7.3$
B	$1.75 \pm 0.25$	$1.9 \pm 4.0$
V	$1.59 \pm 0.15$	$5.9 \pm 2.7$
R	$1.56 \pm 0.10$	$2.4 \pm 1.9$
I	$1.33 \pm 0.18$	$2.1 \pm 3.9$
Star 18 (mP)		
U	$1.64 \pm 0.19$	$7.6 \pm 3.3$
B	$1.87 \pm 0.15$	$7.7 \pm 2.3$
V	$1.89 \pm 0.18$	$7.5 \pm 2.7$
R	$1.90 \pm 0.15$	$5.9 \pm 2.2$
I	$1.36 \pm 0.20$	$6.1 \pm 4.3$

**Table 2.** continued

Star Id. Filter	$P_\lambda \pm \epsilon_P$ %	$\theta_\lambda \pm \epsilon_\theta$ °
Star 19		
U	$1.29 \pm 0.31$	$178.3 \pm 6.6$
B	$2.32 \pm 0.10$	$177.5 \pm 1.3$
V	$2.30 \pm 0.12$	$175.4 \pm 1.5$
R	$2.43 \pm 0.09$	$175.4 \pm 1.0$
I	$2.11 \pm 0.11$	$176.0 \pm 1.5$
Star 20 (nP)		
U	$1.36 \pm 0.23$	$7.1 \pm 4.8$
B	$1.67 \pm 0.13$	$4.2 \pm 2.3$
V	$1.57 \pm 0.14$	$2.7 \pm 2.5$
R	$1.61 \pm 0.12$	$2.6 \pm 2.2$
I	$1.48 \pm 0.16$	$0.3 \pm 3.2$
Star 21 (mP)		
U	$1.94 \pm 0.35$	$5.1 \pm 5.1$
B	$2.33 \pm 0.10$	$5.0 \pm 1.3$
V	$2.27 \pm 0.10$	$3.2 \pm 1.2$
R	$2.40 \pm 0.06$	$4.6 \pm 0.8$
I	$2.24 \pm 0.09$	$5.6 \pm 1.2$
Star 22 (nP)		
U	$2.06 \pm 0.47$	$7.4 \pm 6.5$
B	$2.36 \pm 0.16$	$3.2 \pm 1.9$
V	$2.41 \pm 0.15$	$5.5 \pm 1.8$
R	$2.46 \pm 0.13$	$5.0 \pm 1.5$
I	$2.32 \pm 0.15$	$5.2 \pm 1.9$
Star 23 (P)		
U	$1.53 \pm 0.20$	$4.9 \pm 3.8$
B	$1.65 \pm 0.12$	$7.4 \pm 2.1$
V	$1.82 \pm 0.13$	$5.3 \pm 2.1$
R	$1.76 \pm 0.09$	$3.8 \pm 1.5$
I	$1.60 \pm 0.13$	$1.8 \pm 2.4$
Star 24 (mP)		
U	$1.63 \pm 0.21$	$0.0 \pm 3.6$
B	$1.95 \pm 0.16$	$3.5 \pm 2.4$
V	$2.05 \pm 0.12$	$4.0 \pm 1.6$
R	$2.07 \pm 0.13$	$2.4 \pm 1.8$
I	$1.75 \pm 0.18$	$1.8 \pm 3.0$
Star 25		
U	$1.48 \pm 0.16$	$10.8 \pm 3.0$
B	$1.71 \pm 0.07$	$12.4 \pm 1.2$
V	$1.65 \pm 0.08$	$12.2 \pm 1.4$
R	$1.72 \pm 0.06$	$10.7 \pm 0.9$
I	$1.43 \pm 0.10$	$10.6 \pm 2.0$
Star 26 (nP)		
U	$2.08 \pm 0.33$	$179.8 \pm 4.5$
B	$2.46 \pm 0.30$	$7.0 \pm 3.5$
V	$2.44 \pm 0.40$	$11.9 \pm 4.6$
R	$2.30 \pm 0.34$	$11.1 \pm 4.2$
I	$2.09 \pm 0.33$	$12.1 \pm 4.5$
Star 27		
U	$0.88 \pm 0.19$	$19.8 \pm 5.9$
B	$1.05 \pm 0.10$	$9.7 \pm 2.7$
V	$1.19 \pm 0.12$	$6.3 \pm 3.0$
R	$1.25 \pm 0.16$	$5.6 \pm 3.7$
I	$1.08 \pm 0.17$	$3.4 \pm 4.5$

Table 2. continued

Star Id. Filter	$P_\lambda \pm \epsilon_P$ %	$\theta_\lambda \pm \epsilon_\theta$ °
Star 28 (nP)		
U	$1.91 \pm 0.37$	$3.9 \pm 5.4$
B	$1.88 \pm 0.15$	$3.2 \pm 2.3$
V	$1.84 \pm 0.14$	$0.8 \pm 2.3$
R	$1.85 \pm 0.09$	$1.8 \pm 1.4$
I	$1.68 \pm 0.12$	$4.4 \pm 2.1$
Star 29 (rgP)		
U	$1.55 \pm 1.27$	$34.2 \pm 19.6$
B	$2.07 \pm 0.30$	$2.5 \pm 4.1$
V	$2.22 \pm 0.17$	$2.9 \pm 2.2$
R	$2.24 \pm 0.20$	$2.4 \pm 2.5$
I	$1.89 \pm 0.21$	$1.5 \pm 3.2$
Star 30 (m)		
U	$2.09 \pm 0.34$	$5.3 \pm 4.6$
B	$2.49 \pm 0.20$	$9.5 \pm 2.3$
V	$2.46 \pm 0.15$	$6.4 \pm 1.7$
R	$2.45 \pm 0.13$	$9.1 \pm 1.5$
I	$1.98 \pm 0.26$	$10.7 \pm 3.7$
Star 31		
U	$0.54 \pm 0.34$	$32.2 \pm 16.1$
B	$0.03 \pm 0.12$	$25.3 \pm 39.2$
V	$0.07 \pm 0.13$	$77.6 \pm 30.4$
R	$0.06 \pm 0.14$	$70.1 \pm 33.5$
I	$0.16 \pm 0.15$	$99.3 \pm 21.1$
Star 32 (mP)		
U	$0.94 \pm 0.36$	$16.5 \pm 10.6$
B	$0.97 \pm 0.22$	$13.5 \pm 6.2$
V	$1.02 \pm 0.14$	$6.9 \pm 3.9$
R	$1.04 \pm 0.10$	$11.0 \pm 2.6$
I	$0.69 \pm 0.20$	$2.7 \pm 8.2$
Star 33 (rg)		
U	$2.54 \pm 0.65$	$3.6 \pm 7.2$
B	$2.96 \pm 0.18$	$16.7 \pm 1.7$
V	$2.78 \pm 0.11$	$15.8 \pm 1.1$
R	$2.90 \pm 0.09$	$16.6 \pm 0.9$
I	$2.48 \pm 0.09$	$15.4 \pm 1.0$
Star 34 (n)		
U	$1.64 \pm 0.25$	$22.6 \pm 4.4$
B	$2.66 \pm 0.13$	$14.7 \pm 1.4$
V	$2.46 \pm 0.13$	$17.2 \pm 1.5$
R	$2.65 \pm 0.12$	$16.1 \pm 1.3$
I	$2.24 \pm 0.16$	$15.3 \pm 2.1$
Star 35 (rg)		
U	$1.49 \pm 0.49$	$1.6 \pm 9.0$
B	$2.48 \pm 0.11$	$2.8 \pm 1.3$
V	$2.39 \pm 0.11$	$4.9 \pm 1.3$
R	$2.49 \pm 0.08$	$4.4 \pm 0.9$
I	$2.18 \pm 0.10$	$4.0 \pm 1.3$
Star 36 (rg)		
U	$4.52 \pm 1.25$	$16.0 \pm 7.7$
B	$2.38 \pm 0.25$	$20.7 \pm 3.0$
V	$2.17 \pm 0.20$	$28.2 \pm 2.6$
R	$2.33 \pm 0.22$	$27.9 \pm 2.7$
I	$2.12 \pm 0.23$	$31.7 \pm 3.1$

**Table 2.** continued

Star Id. Filter	$P_\lambda \pm \epsilon_P$ %	$\theta_\lambda \pm \epsilon_\theta$ °
Star 37 (mP)		
U	$1.84 \pm 0.37$	$13.0 \pm 5.6$
B	$2.27 \pm 0.21$	$11.9 \pm 2.6$
V	$2.40 \pm 0.13$	$10.1 \pm 1.6$
R	$2.39 \pm 0.11$	$8.0 \pm 1.3$
I	$2.25 \pm 0.17$	$6.5 \pm 2.2$
Star 38 (mP)		
U	$1.21 \pm 0.21$	$3.5 \pm 4.9$
B	$1.51 \pm 0.12$	$9.7 \pm 2.3$
V	$1.71 \pm 0.09$	$9.0 \pm 1.6$
R	$1.64 \pm 0.08$	$9.8 \pm 1.4$
I	$1.58 \pm 0.14$	$7.2 \pm 2.4$
Star 39 (nP)		
U	$1.74 \pm 0.19$	$18.6 \pm 3.2$
B	$2.20 \pm 0.10$	$19.7 \pm 1.3$
V	$2.11 \pm 0.09$	$17.2 \pm 1.2$
R	$2.20 \pm 0.07$	$17.2 \pm 0.9$
I	$2.06 \pm 0.09$	$15.2 \pm 1.3$
Star 40 (mP)		
U	$2.66 \pm 0.44$	$15.7 \pm 4.6$
B	$1.91 \pm 0.17$	$11.5 \pm 2.6$
V	$2.07 \pm 0.11$	$11.7 \pm 1.5$
R	$2.10 \pm 0.07$	$11.0 \pm 0.9$
I	$1.84 \pm 0.15$	$11.3 \pm 2.4$
Star 41 (rg)		
U	$2.31 \pm 1.15$	$22.7 \pm 13.2$
B	$1.85 \pm 0.27$	$5.6 \pm 4.2$
V	$1.58 \pm 0.23$	$10.2 \pm 4.1$
R	$1.69 \pm 0.26$	$11.5 \pm 4.4$
I	$1.58 \pm 0.28$	$11.5 \pm 5.1$
Star 42 (mP)		
U	$2.21 \pm 0.22$	$17.2 \pm 2.9$
B	$2.45 \pm 0.18$	$18.7 \pm 2.1$
V	$2.13 \pm 0.08$	$17.6 \pm 1.0$
R	$2.27 \pm 0.11$	$17.2 \pm 1.4$
I	$2.13 \pm 0.11$	$16.4 \pm 1.5$
Star 43 (m)		
U	$2.26 \pm 0.21$	$14.7 \pm 2.6$
B	$2.82 \pm 0.18$	$17.7 \pm 1.8$
V	$2.97 \pm 0.12$	$18.1 \pm 1.2$
R	$3.04 \pm 0.11$	$17.9 \pm 1.0$
I	$2.77 \pm 0.16$	$19.1 \pm 1.7$
Star 44 (n)		
U	$1.32 \pm 0.16$	$14.7 \pm 3.5$
B	$1.80 \pm 0.12$	$12.0 \pm 1.8$
V	$1.71 \pm 0.23$	$15.3 \pm 3.8$
R	$1.82 \pm 0.20$	$15.3 \pm 3.1$
I	$1.63 \pm 0.15$	$17.0 \pm 2.7$
Star 45 (n)		
U	$1.12 \pm 0.31$	$20.0 \pm 7.8$
B	$1.56 \pm 0.17$	$19.7 \pm 3.0$
V	$1.62 \pm 0.14$	$18.6 \pm 2.5$
R	$1.67 \pm 0.12$	$20.2 \pm 2.1$
I	$1.38 \pm 0.23$	$16.0 \pm 4.8$

**Table 2.** continued

Star Id. Filter	$P_\lambda \pm \epsilon_P$ %	$\theta_\lambda \pm \epsilon_\theta$ °
Star 46		
U	$1.50 \pm 0.18$	$34.0 \pm 3.5$
B	$1.73 \pm 0.12$	$24.4 \pm 1.9$
V	$1.78 \pm 0.17$	$20.0 \pm 2.7$
R	$1.86 \pm 0.13$	$20.7 \pm 2.0$
I	$1.70 \pm 0.16$	$17.0 \pm 2.7$

m: member (determination from the literature, see text)

n: non-member

rg: red giant

P: observed by Pedreros (1987)

**Table 3.** Parameters of the Serkowski's fit to the linear polarization data for stars in NGC 6124

Stellar Identification	$P_{max} \pm \epsilon_P$ %	$\sigma_1^a$	$\lambda_{max} \pm \epsilon_{\lambda_{max}}$ m $\mu$	$\bar{\epsilon}$
1	3.753 $\pm$ 0.182	1.392	0.567 $\pm$ 0.063	0.85
2	3.636 $\pm$ 0.090	1.061	0.559 $\pm$ 0.024	0.38
3	0.974 $\pm$ 0.024	0.543	0.614 $\pm$ 0.033	0.23
4	3.538 $\pm$ 0.088	1.266	0.595 $\pm$ 0.033	0.93
5	2.826 $\pm$ 0.035	0.494	0.592 $\pm$ 0.015	0.34
7	2.252 $\pm$ 0.047	0.354	0.483 $\pm$ 0.016	1.06
8	2.062 $\pm$ 0.051	0.849	0.552 $\pm$ 0.029	0.55
10	1.867 $\pm$ 0.040	0.266	0.526 $\pm$ 0.021	3.51
11	3.093 $\pm$ 0.020	0.312	0.576 $\pm$ 0.008	0.58
12	2.366 $\pm$ 0.082	0.641	0.617 $\pm$ 0.042	1.49
13	1.894 $\pm$ 0.043	0.428	0.576 $\pm$ 0.025	9.06
14	2.646 $\pm$ 0.127	0.901	0.539 $\pm$ 0.054	0.40
15	2.644 $\pm$ 0.059	0.745	0.572 $\pm$ 0.026	0.62
16	1.633 $\pm$ 0.029	0.541	0.562 $\pm$ 0.022	0.57
17	1.714 $\pm$ 0.075	0.620	0.488 $\pm$ 0.036	0.70
18	1.895 $\pm$ 0.070	0.781	0.512 $\pm$ 0.037	0.22
19	2.400 $\pm$ 0.101	1.489	0.605 $\pm$ 0.057	0.33
20	1.671 $\pm$ 0.040	0.587	0.560 $\pm$ 0.029	0.85
21	2.435 $\pm$ 0.043	0.943	0.599 $\pm$ 0.025	0.30
22	2.518 $\pm$ 0.027	0.359	0.599 $\pm$ 0.015	0.29
23	1.809 $\pm$ 0.017	0.274	0.575 $\pm$ 0.011	1.28
24	2.065 $\pm$ 0.032	0.430	0.581 $\pm$ 0.020	0.53
25	1.749 $\pm$ 0.038	0.970	0.546 $\pm$ 0.026	0.57
26	2.465 $\pm$ 0.031	0.192	0.539 $\pm$ 0.012	4.84
27	1.206 $\pm$ 0.024	0.283	0.642 $\pm$ 0.021	3.85
28	1.942 $\pm$ 0.044	0.588	0.546 $\pm$ 0.025	0.58
29	2.232 $\pm$ 0.048	0.393	0.564 $\pm$ 0.028	0.83
30	2.514 $\pm$ 0.053	0.558	0.538 $\pm$ 0.026	0.81
32	1.050 $\pm$ 0.099	0.799	0.516 $\pm$ 0.099	1.41
33	2.930 $\pm$ 0.084	1.181	0.551 $\pm$ 0.031	0.44
34	2.613 $\pm$ 0.130	1.715	0.596 $\pm$ 0.065	1.12
35	2.535 $\pm$ 0.065	1.128	0.559 $\pm$ 0.031	0.42
36	2.355 $\pm$ 0.094	0.796	0.576 $\pm$ 0.054	5.06
37	2.441 $\pm$ 0.015	0.185	0.606 $\pm$ 0.009	0.90
38	1.688 $\pm$ 0.025	0.466	0.623 $\pm$ 0.022	0.66
39	2.247 $\pm$ 0.046	1.081	0.593 $\pm$ 0.028	1.18
40	2.145 $\pm$ 0.078	1.310	0.567 $\pm$ 0.052	0.23
41	1.754 $\pm$ 0.098	0.696	0.553 $\pm$ 0.071	1.37
42	2.301 $\pm$ 0.096	1.810	0.576 $\pm$ 0.057	0.23
43	3.045 $\pm$ 0.030	0.402	0.620 $\pm$ 0.013	0.49
44	1.829 $\pm$ 0.074	0.831	0.602 $\pm$ 0.040	1.34
45	1.648 $\pm$ 0.048	0.532	0.606 $\pm$ 0.041	0.34
46	1.871 $\pm$ 0.018	0.254	0.597 $\pm$ 0.011	7.96

a)  $\sigma_1^2 = \sum (r_\lambda / \epsilon_{p_\lambda})^2 / (m - 2)$ ; where  
 $m$  is the number of colors and  
 $r_\lambda = P_\lambda - P_{\max} \exp(-K \ln^2(\lambda_{\max}/\lambda))$

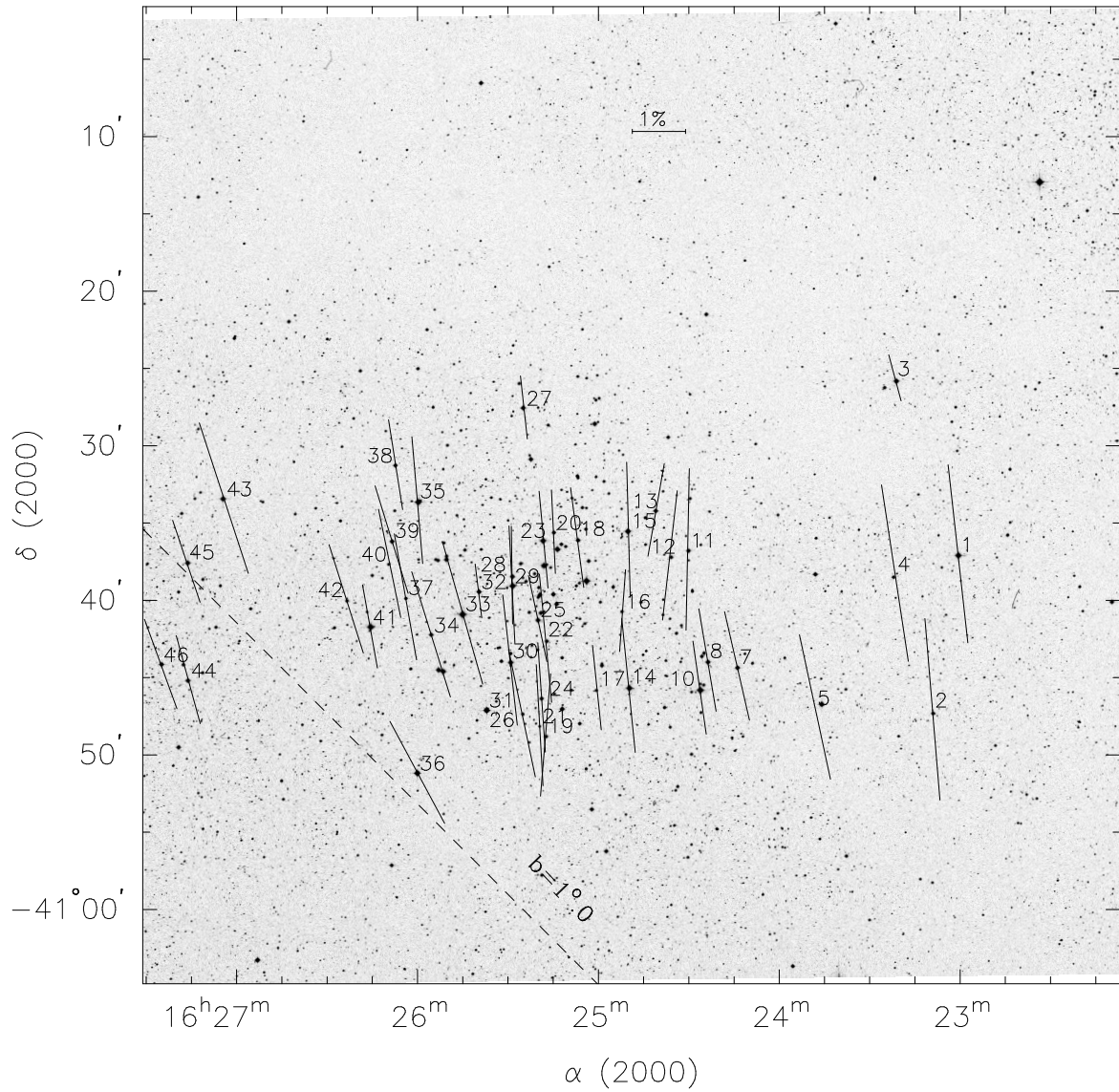


**Figure 1.** Projection on the sky of the polarization vectors (Johnson V filter) of the stars observed in the region of NGC 6124. The dashed line is the galactic parallel  $b = 1^\circ$ . This plot shows only the observed stars close to the central core.

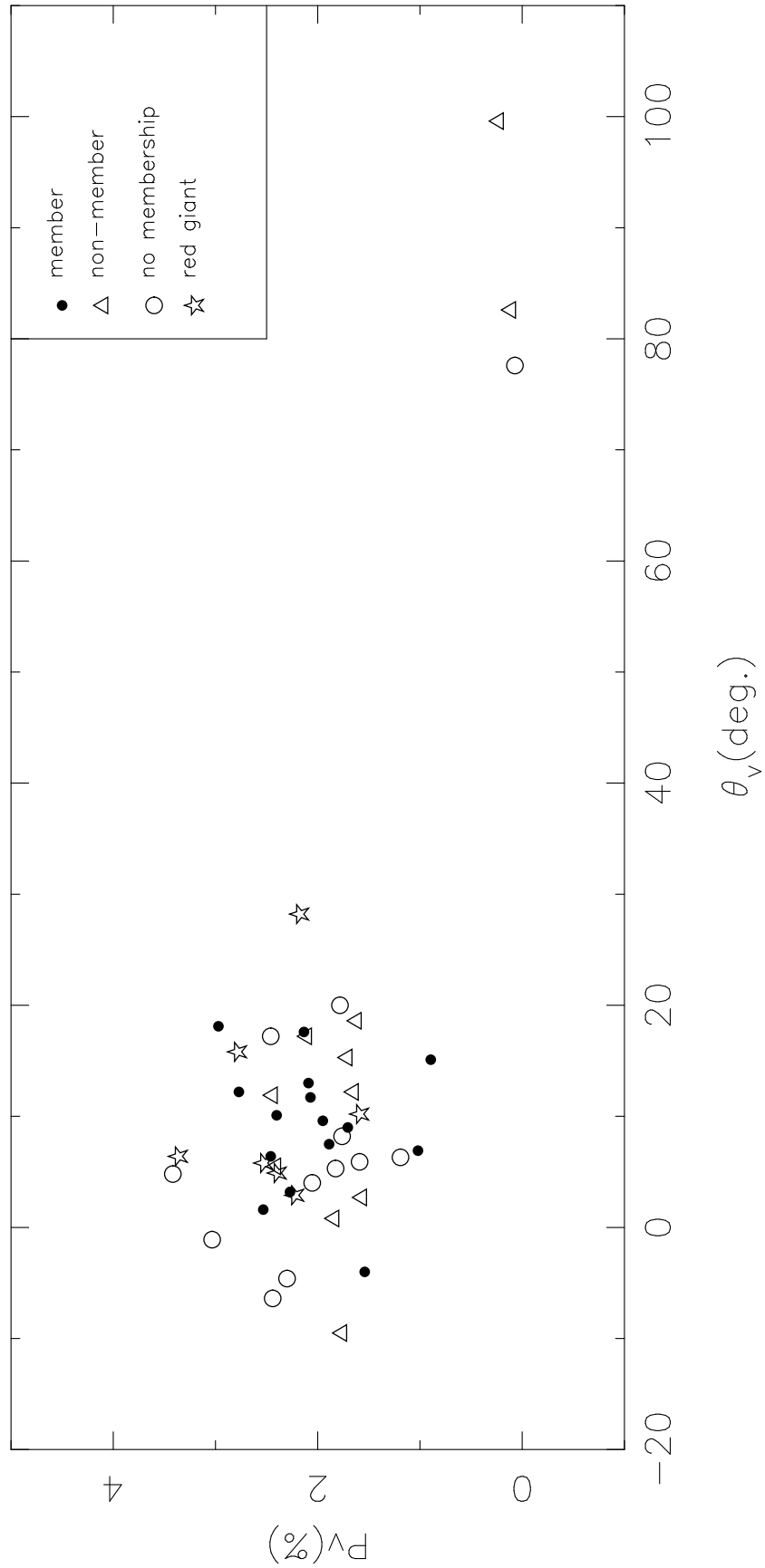


**Figure 2.** V-band polarization percentage of the stellar flux  $P_V$  (%) vs. the polarization angle  $\theta_V$  for each star. Symbols indicate the membership classification from the literature. No membership means that there are not previous membership studies.

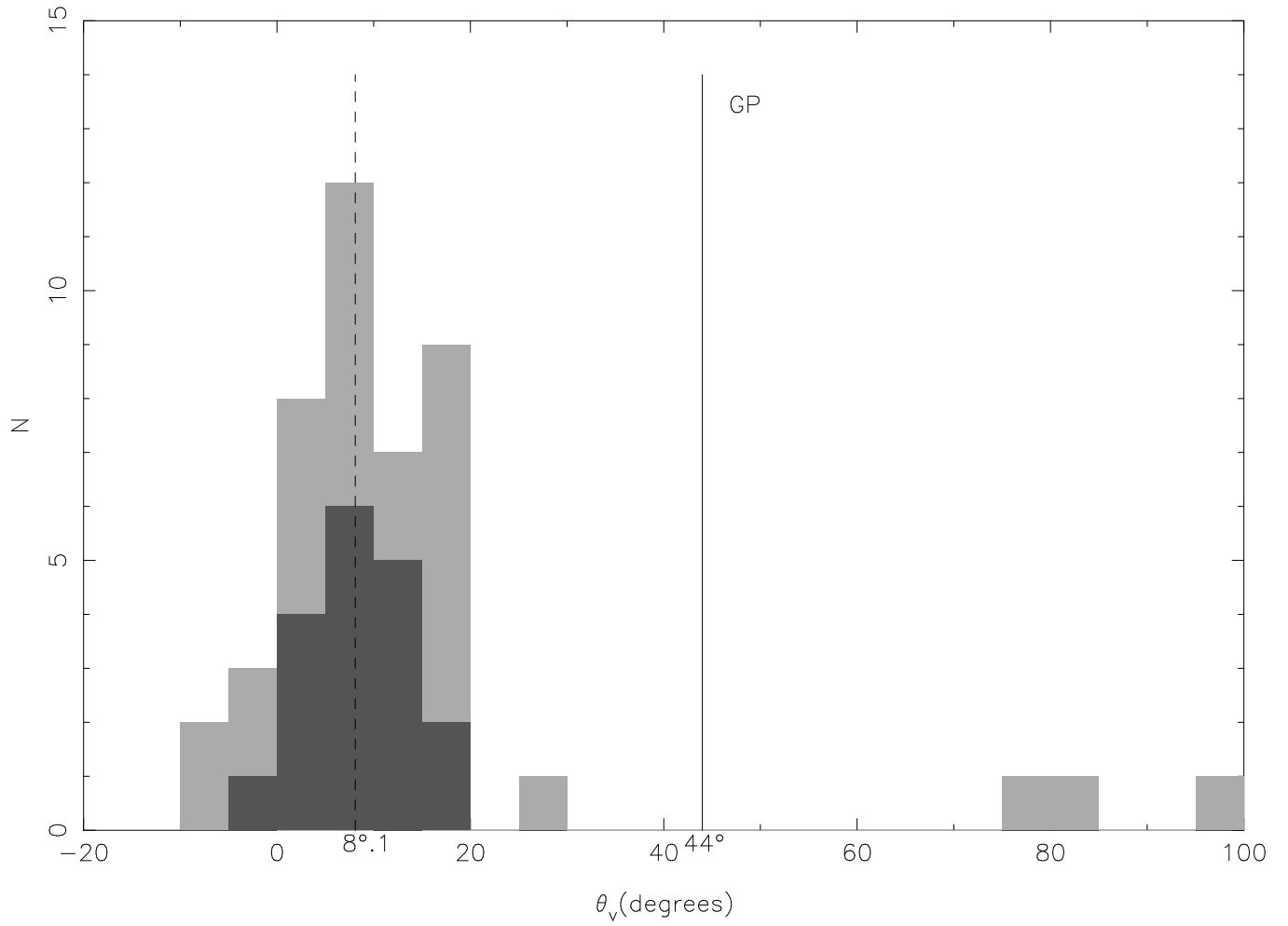


**Figure 3.** Polarization angle distribution. Grey bars are the histogram for all the stars observed in the region, while the dark ones are for the member stars. The solid line, labeled as GP, is the projection of the Galactic Plane in the region and the dashed line is the average angle of the polarization vector for the cluster.

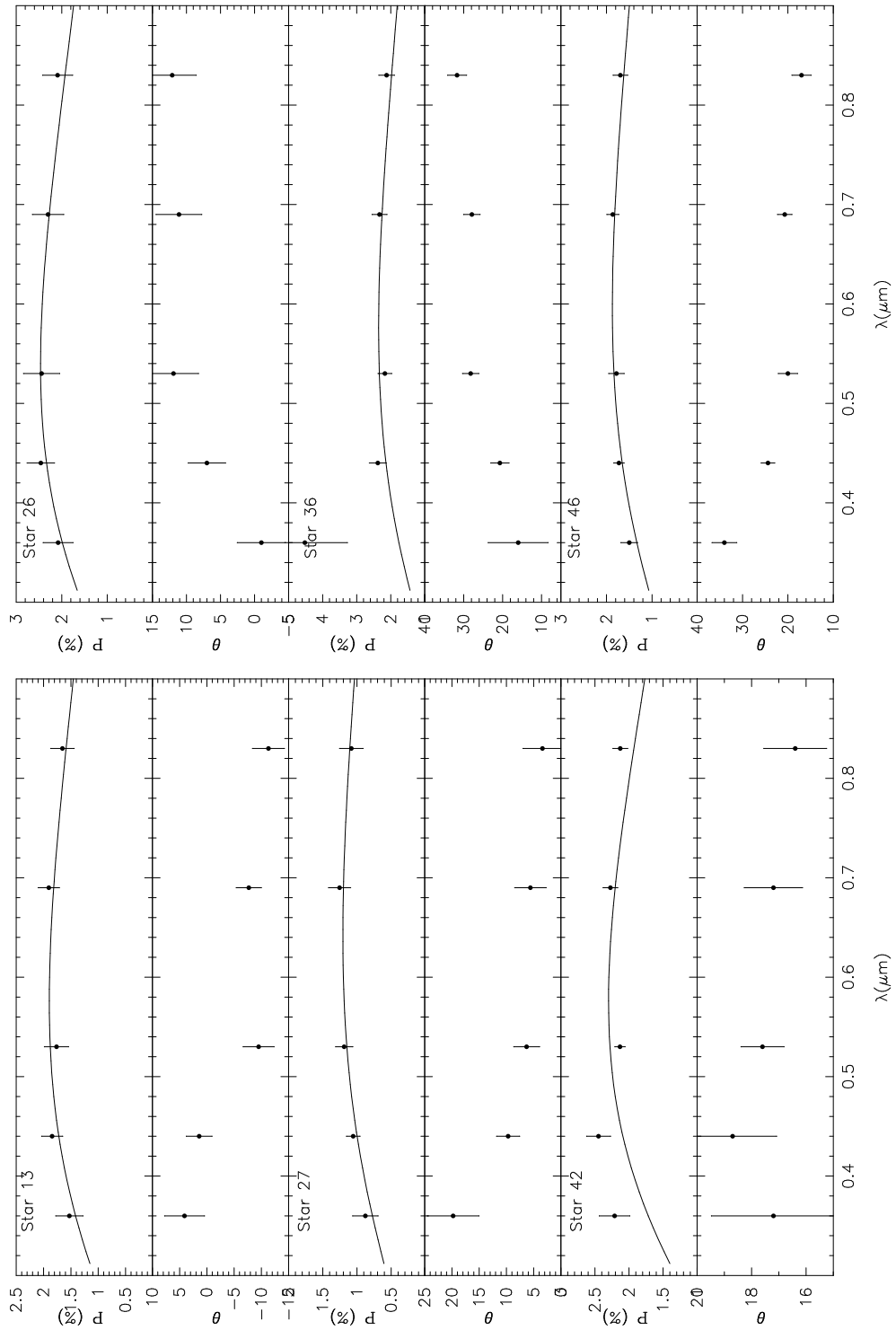


**Figure 4.** Polarization and position angle dependence on wavelength for stars with features of intrinsic polarization

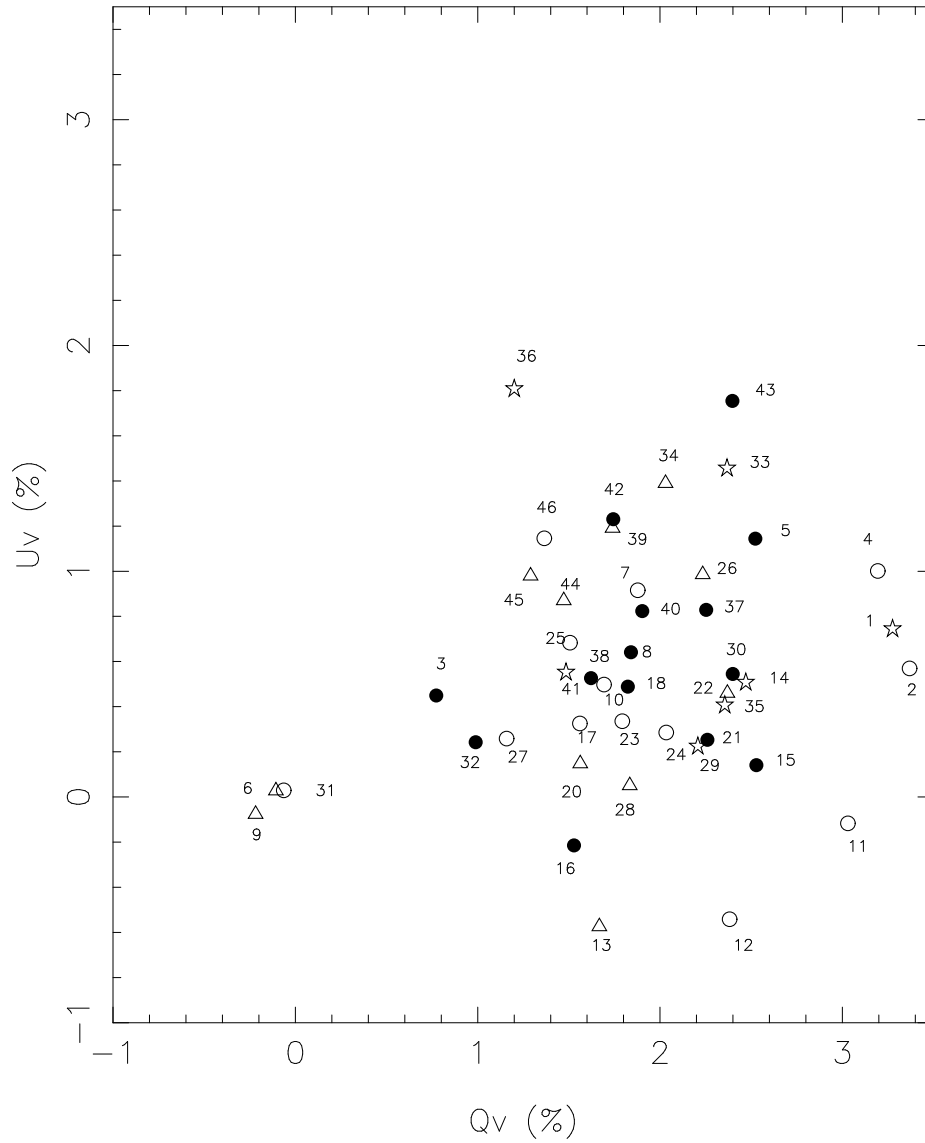


**Figure 5.**  $U_V$  vs.  $Q_V$  plot for the stars in the region of NGC 6124. Symbols are as in Fig. 2.

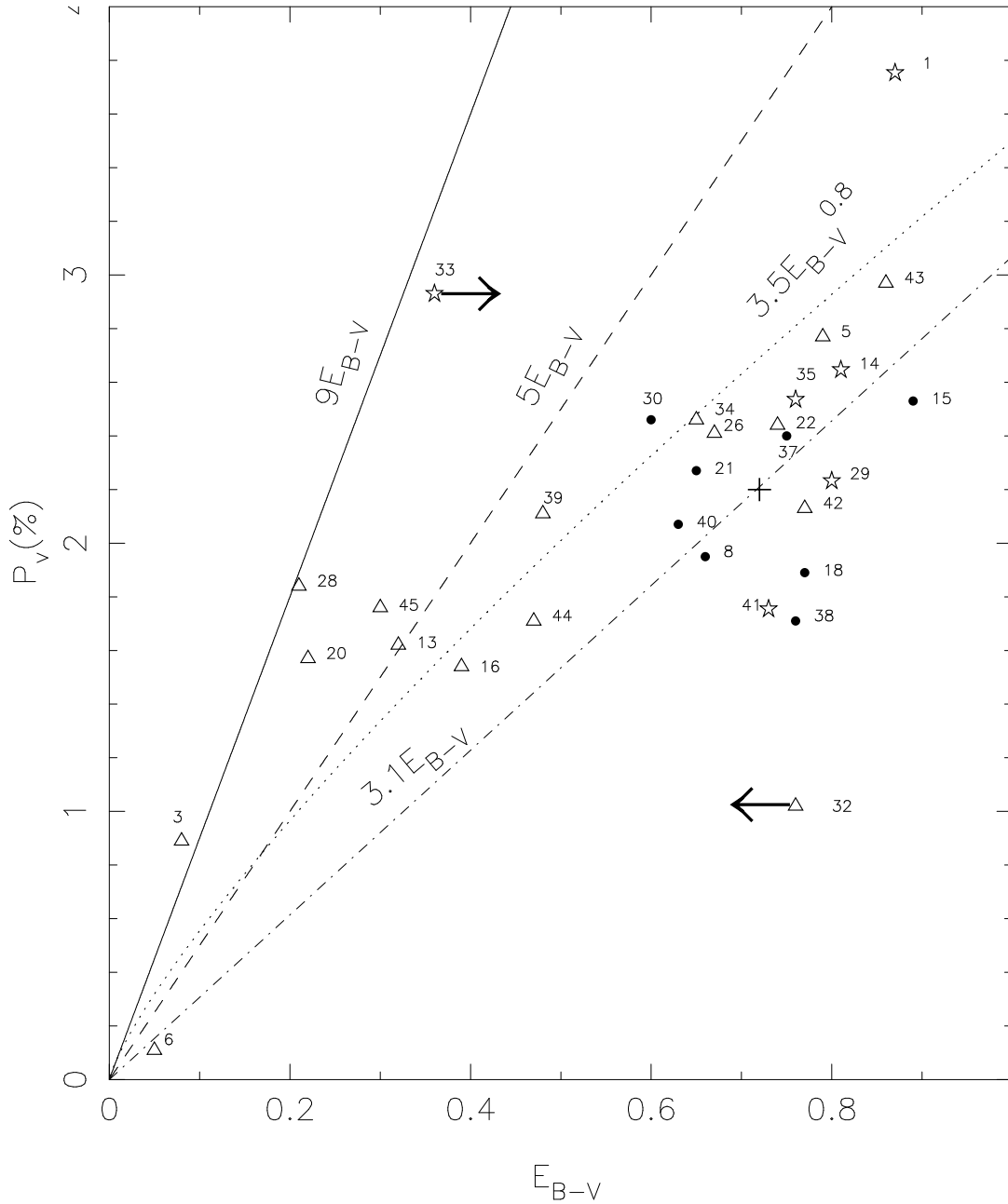


**Figure 6.** Plot  $P_V$  vs.  $E_{B-V}$  for stars in the region of NGC 6124. From left to right the solid line is the maximum polarimetric efficiency  $P_V = 9E_{B-V}$ , the dashed line is the Serkowski's estimate average for the Galaxy  $P_V = 5E_{B-V}$ , the dotted line is the Fosalba's estimate  $P_V = 3.5E(B - V)^{0.8}$ , and the dot-dashed line is the efficiency found for the cluster  $P_V = 3.1E_{B-V}$ . Symbols are as in Fig. 2, but the memberships were modified as discussed in section 4.2.

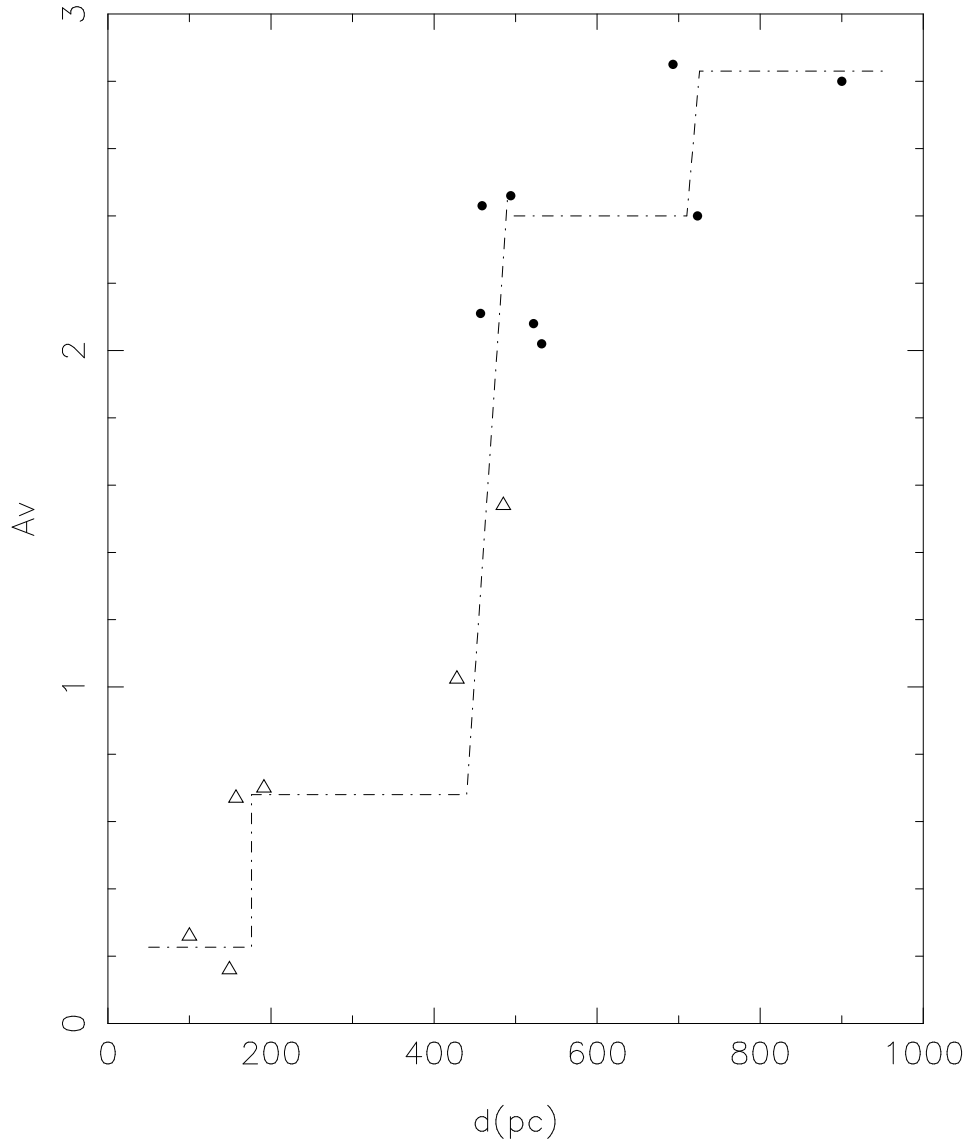


**Figure 7.** Variation of the absorption ( $A_V$ ) with increasing distance in the area of NGC 6124. This figure includes only those stars whose distances could be estimated. Open triangles are non-members and solid circles are members.